Omnidirectional negative refraction with wide bandwidth introduced by magnetic coupling in a tri-rod structure

Fu-Ming Wang,[1] Hui Liu,[1] Tao Li,[1] Shi-Ning Zhu,[1,*] and Xiang Zhang[2]
[1]*Department of Physics, National Laboratory of Solid State Microstructures, Nanjing University, Nanjing 210093, People's Republic of China*
[2]*Nanoscale Science and Engineering Center, University of California, 5130 Etcheverry Hall, Berkeley, California 94720-1740, USA*
(Received 13 April 2007; revised manuscript received 20 July 2007; published 9 August 2007)

A tri-rod structure, which can be seen as a combination of nanorod pairs reported by Shalaev *et al.* [Opt. Lett. **30**, 3356 (2005)], is proposed to realize negative refractions at infrared frequencies. In this system, a magnetic coupling effect is found between the two nanopairs and it results in two magnetic resonance modes: one mode at 146.6 THz and the other mode at 154.1 THz. The retrieved effective indices from scattering (*S*) parameters show that this coupling effect plays an important role in improving the negative property of the metamaterial. It can help to realize omnidirectional negative refractions and broaden the bandwidth of negative refraction. Metamaterials composed from tri-rod elements are used to simulate the negative-refraction behaviors of the electromagnetic wave with different propagation directions, providing direct evidence for the retrieved results.

DOI: 10.1103/PhysRevB.76.075110 PACS number(s): 41.20.Jb, 78.20.Ci, 73.20.Mf

Since left-handed material (LHM) consisting of split-ring resonators[1] and continuous wires[2] was first demonstrated experimentally at the microwave region in 2000,[3] artificial materials with negative-refractive index[4–10] or only negative permeability[11–17] have attracted more and more attention of researchers all over the world. LHMs usually include magnetic and electric components, which provide negative permeability and negative permittivity, respectively. Similar to the atoms arranged periodically in natural crystals, magnetic resonant elements in metamaterials can be seen as artificial "magnetic atoms."[15] In such a unit, a closed *LC* circuit is formed, and the inductive currents provide strong magnetic moment at resonance frequency.

Very recently, in order to increase the frequency of negative index, some new structures, such as "double-fishnet" structures,[8–10] have been designed to realize negative refractions at wavelength 780 nm. Periodic array of pairs of thin silver strips is employed to get negative permeability at red light.[11] Direct evidence for negative refraction in nanorod-pair systems was also obtained when an *S*-polarized electromagnetic (EM) wave propagates along the substrate surface.[7] However, for the above systems, negative index is only proven for the normal incident case. If EM wave is shined on the sample with different directions, what will happen to the negative-refraction property? Actually, the negative-refractive indices of these structures are deeply dependent on the propagation direction of the EM wave. The strongest magnetic resonance is attained for the normal-incidence case. If we tilt the incident angle, the strength of magnetic response will decrease rapidly and disappear completely at 90° incident angle. Though omnidirectional negative refractions (ONRs) have been reported in photonics crystals,[18–20] realization of ONR in LHM, especially at optical frequencies, is still a challenging problem.[21]

Besides the increasing frequency requirement, the narrow bandwidth of negative index is another obstacle for the application of LHM. As for all magnetic resonant structures reported up to now, the resonant peak is very narrow and negative permeability is limited in a very small frequency range. This property is an unignored disadvantage for LHM, especially for negative refraction at different color light. Can we find a mechanism to broaden the bandwidth of negative refraction?

In the natural world, each isolated atom has discrete energy levels at certain frequencies. One molecule, composed of the atoms, will possess more energy levels due to the interaction between these atoms. The same thing would happen in metamaterial. The double-rod system (DRS), which was first invented by Shalaev *et al.*,[6] can be seen as a kind of artificial magnetic atom. In this paper, we will propose a tri-rod system (TRS), which is combined of two pairs of nanorods and can behave like a magnetic molecule. As for DRS, there is only one resonance frequency at which the negative permeability is obtained. For our system, strong coupling can be established between two nanorod pairs. As a result, the original magnetic resonance level is split into two levels corresponding to two different resonance modes. With omnidirectional incidence of the EM wave in the *xy* plane and the electric field polarized along the *z* axis, ONR can be realized in this structure. Additionally, as the two resonant levels overlap with each other, a broadened negative-refraction bandwidth can be attained simultaneously.

The cubic unit cell of the TRS is shown in Fig. 1(a), which is constituted from three rods A, B, and C. In the simulation, polarized EM wave propagates in the *y* direction, with magnetic field in the *x* direction and electric field in the *z* direction (along the rod). The boundaries of the cube are defined as periodic boundary conditions, which mimic an infinite system with the cube as a unit cell. For comparison, we also investigate DRS for comparison purposes in the following, which composes only two rods: A and B.

To study the EM response of the proposed TRS, we perform a set of finite-difference time-domain calculations using a commercial software package CST MICROWAVE STUDIO (Computer Simulation Technology GmbH, Darmstadt, Germany). In the calculations, we rely on the Drude model to

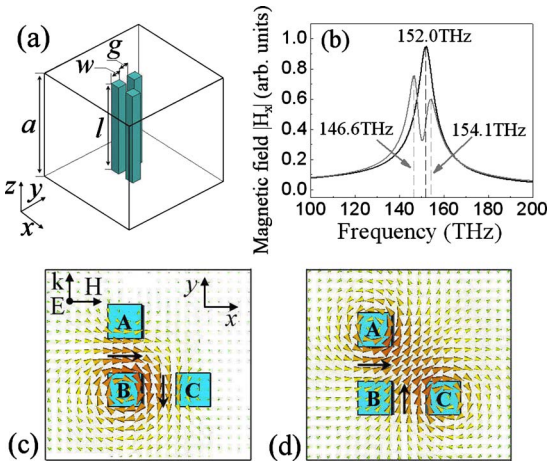

FIG. 1. (Color online) (a) The schematic illustration of a cubic unit cell of the TRS with $a=600$ nm, $l=500$ nm, $w=50$ nm, and $g=50$ nm. The rod cross section is square. (b) The detected magnetic field amplitude $|H_x|$ between rods A and B for the TRS (gray curve) and DRS (black curve) is plotted versus the frequencies. The magnetic field vector distributions at (c) 146.6 THz and (d) 154.1 THz are shown on the xy plane, with the EM wave propagating along the y axis. The long black arrows between the rods represent the directions of magnetic moments.

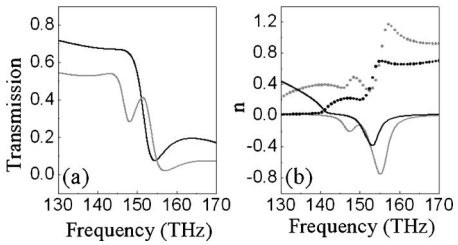

FIG. 2. (a) Transmission spectra for one unit cell of the TRS (gray curve), and DRS (black curve) with the EM wave propagating along the y axis. (b) Retrieved effective refractive indices for TRS (gray curve) and DRS (black curve). The continuous and dotted curves represent the real and imaginary parts, respectively.

characterize the bulk metal properties. Namely, the metal permittivity in the infrared spectral range is given by $\varepsilon=1-\omega_p^2/(\omega^2+i\omega\gamma)$, where ω_p is the bulk plasma frequency and γ is the relaxation rate. For gold, the characteristic frequencies fitted to experimental data are $\omega_p=1.37\times10^{16}$ s^{-1} and $\gamma=4.08\times10^{13}$ s^{-1}.[22]

In our simulations, a probe is placed between rods A and B to detect the local magnetic field. The recorded magnetic field amplitude $|H_x|$ is presented in Fig. 1(b). The intensity of the magnetic field is enhanced greatly at certain frequencies, which indicates that strong magnetic resonance occurs at these frequencies. Obviously, there is only one resonance peak for the DRS, which occurs at 152.0 THz [see Fig. 1(b), black curve]. As for TRS [see Fig. 1(b), gray curve], the original single peak of DRS splits into two resonance peaks: one at 146.6 THz and the other at 154.1 THz. The frequency range of these two peaks overlaps at about 150 THz.

To further study how the magnetic atoms couple with each other, we calculate the magnetic field vector distributions in the xy plane at the two resonance modes of TRS, as shown in Figs. 1(c) and 1(d). The long black arrows between the rods schematically represent the directions of the magnetic moments. In both modes, strong magnetic moments can be formed at the centers of two magnetic atoms. Further calculation of the local current distributions in the rods shows that the currents in rod B contribute to the two magnetic atoms in the TRS simultaneously. The exchange of the conduction current through rod B between two resonant magnetic atoms leads to strong magnetic coupling.[23] Additionally, we can also see that large overlapping of magnetic field from the two magnetic atoms occurs in the unit cell, which results in another kind of interaction, magnetoinductive coupling.[24] These two kinds of magnetic coupling work together to broaden negative-refraction bandwidth.

In order to retrieve the effective index of TRS, the unit cell is put in a waveguide, with the size shown as the frame in Fig. 1(a). Transmission spectra for one unit cell of the TRS (gray curve) and DRS (black curve) are presented in Fig. 2(a). Using the S-parameter retrieval methods,[25] we extract the refractive indices of the TRS (gray curve) and DRS (black curve) [see Fig. 2(b)]. The continuous curves and dotted curves represent the real and imaginary parts, respectively. Obviously, as for the TRS, much broader negative index bandwidth is obtained. The overlapping of the two resonance modes in the TRS leads to a continuous transition of the real part curve at about 150 THz. As a result, the bandwidth of negative refraction is broadened from 18.3 to 31.8 THz as compared to the DRS under normal incidence. For TRS, with the broader bandwidth, the magnetic response becomes weaker correspondingly. However, as is well known, the value of the refractive index is determined by the permittivity and the permeability simultaneously. Because more metal material is enclosed in the unit cell of TRS, its permittivity is more negative than that of DRS. From the simulation results, we found that the change of permittivity dominates over the change of permeability. So the value of the real part of the refractive index for the TRS is more negative than that for the DRS. Furthermore, the important LHM quality, figure of merit [FOM$=|\mathrm{Re}(n)/\mathrm{Im}(n)|$] of the TRS reaches about 1.42, which is also larger than that of DRS (FOM$=1.07$).

Similar to most artificial magnetic resonators, the optical response of DRS is polarization dependent. The magnetic response would become much weaker under oblique angle to the rod-gap-rod plane. If the EM wave propagates perpendicularly to the rod-gap-rod plane, no magnetic field penetrates the gap between two rods and magnetic response will disappear completely. In the TRS, the orthogonal array of the two magnetic atoms makes the magnetic response excited under any incidence angle. We calculate the refractive indices of the TRS with the EM wave propagating along x, $-x$, y, and $-y$, respectively. Both the real and imaginary parts of the refractive indices in the four cases coincide very well.

However, what we are most interested in is whether negative refraction is always realizable at any propagation direction, which is more important for the actual applications. To

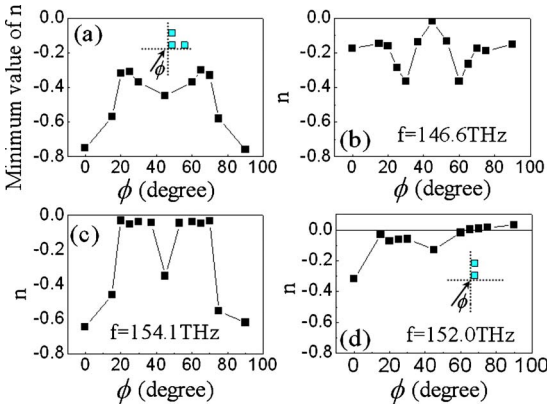

FIG. 3. (Color online) (a) The minimum values of n under different incidence angles. (b) and (c) are refractive indices of TRS at 146.6 and 154.1 THz, respectively. (d) is the refractive index of DRS at 152.0 THz. The insets in (a) and (d) are the schematic illustrations of the wave incidence at an oblique angle. The arrow represents the propagation direction of the wave.

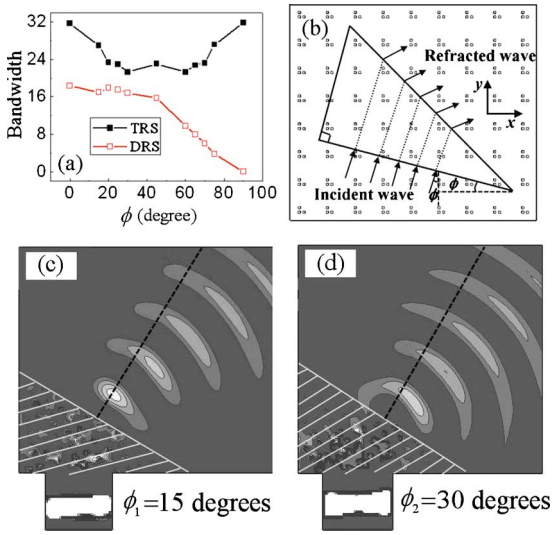

FIG. 4. (Color online) (a) The negative-refraction bandwidth vs the incidence angle of the TRS (black curve with closed squares) and DRS [red (dark gray) curve with hollow squares]. (b) The selection of the wedges for the simulations. The typical magnitude distributions of electric field for negative refractions in the wedges are shown with (c) $\phi_1=15°$ and (d) $\phi_2=30°$.

calculate the S parameters under different incidence angles, we rotate the TRS with a required angle around the z axis in the waveguide, with geometric parameters of the rods unchanged. The EM wave keeps the same propagation direction. So it can enter the TRS at a designed angle. From the S parameters for one unit cell, we retrieve the negative refractive indices of the TRS under different incidence angles. Figure 3(a) shows the relation between the minimum values of Re(n) (in the range from 140 to 160 THz) and the incidence angles ϕ. As TRS has structural symmetry relative to $\phi=45°$ incident direction, the values of Re(n) should have the same symmetry property, which plays a significant role in the realization of ONR. Furthermore, at the two eigenfrequencies of the TRS, 146.6 and 154.1 THz, the refractive indices are shown in Figs. 3(b) and 3(c), respectively. It is obviously seen that ONR is realized at both frequencies. Further investigations show that ONR is attained for all frequencies from 143.3 to 159.2 THz. Simulations were also done for DRS for comparison. It is found that refractive index depends on the incidence angle greatly. At the resonance eigenfrequency of 152.0 THz, no negative value can be achieved if the incidence angle is larger than 65° [see FIG. 3(d)].

Figure 4(a) shows the frequency bandwidth of negative refractions at different incidence angles for the TRS (black curve with closed squares) and the DRS [red (dark gray) curve with hollow squares]. The smallest negative-refraction bandwidth (21.3 THz) of the TRS is still broader than the largest negative-refraction bandwidth (18.3 THz) of the DRS.

The unit cells can be arrayed periodically in the xy plane to form an infinite two-dimensional artificial effective media [Fig. 4(b), top view]. If the wave enters the effective artificial crystal with an oblique incident angle ϕ relative to the y axis, negative refractions can also be realized in this system. To illustrate it more distinctly, we cut a wedge from the effective media with one right-angle side perpendicular to the incident direction. In this case, the EM wave shines normally on the wedge, which is traditionally used to simulate negative refraction behaviors in LHMs.[7] The wedge is represented as the right triangle area in Fig. 4(b) schematically. The black arrows signify the incident and refracted waves at the first and second interfaces of the wedge, respectively. The results we simulated from the wedges give visible pictures to present the negative-refraction behavior of EM wave propagating in the effective media composed from TRS [see Figs. 4(c) and 4(d)].

In our simulations, the wedges are put between two electrically conducting plates, the spacing between which is one unit cell. We assign the open boundary conditions at the sides of the wedges and the computational domain. This does not influence the behavior of the EM wave propagating through the wedges. The right-angle side of the wedges is put across a rectangular channel, which is used to guide the incident wave shining on the wedge normally at the first interface. Figures 4(c) and 4(d) show the calculated refraction images of electric field distributions at the midplane between the two electrically conducting plates, with ϕ equal to 15° and 30°, respectively. The white lines on the wedges represent the array directions of the unit cells. The angle between white lines and the first interface of the wedge is equal to ϕ. The dashed black lines indicate the surface normal of the wedges. Obviously, the EM waves are refracted negatively at the second interface in both cases. These give direct evidence for the realization of ONR in the proposed TRS.

In conclusion, a tri-rod structure, which can be seen as a combination of two nanorod pairs, is proposed in this paper. Strong magnetic coupling interaction is established between the two nanorod pairs. In this system, two eigenmodes are found at 146.6 and 154.1 THz. Two resonance frequency bands overlap at about 150 THz, and it results in a broad-

-ened negative-refraction frequency band. Under the different incident direction, the smallest bandwidth (21.3 THz) of TRS is still broader than the largest bandwidth (18.3 THz) of the DRS. In addition, ONR are realized in our system, which originates from the structural symmetry of TRS. The wedge shape structures composed from TRS are constructed, and simulations of negative refraction behaviors with oblique excitation of magnetic resonance of TRS give direct evidence for the ONR.

This work was supported by the State Key Program for Basic Research of China (2004CB619003) and the National Natural Science Foundation of China under Contract Nos. 10534042, 60578034, and 10604029.

*Corresponding author. zhusn@nju.edu.cn

[1] J. B. Pendry, A. J. Holden, D. J. Robbins, and W. J. Stewart, IEEE Trans. Microwave Theory Tech. **47**, 2075 (1999).
[2] J. B. Pendry, A. J. Holden, W. J. Stewart, and I. Youngs, Phys. Rev. Lett. **76**, 4773 (1996).
[3] D. R. Smith, W. J. Padilla, D. C. Vier, S. C. Nemat-Nasser, and S. Schultz, Phys. Rev. Lett. **84**, 4184 (2000).
[4] C. G. Parazzoli, R. B. Greegor, K. Li, B. E. C. Koltenbah, and M. Tanielian, Phys. Rev. Lett. **90**, 107401 (2003).
[5] V. A. Podolskiy, A. K. Sarychev, and V. M. Shalaev, Opt. Express **11**, 735 (2003).
[6] V. M. Shalaev, W. Cai, U. K. Chettiar, H. K. Yuan, A. K. Sarychev, V. P. Drachev, and A. V. Kildishev, Opt. Lett. **30**, 3356 (2005).
[7] F. M. Wang, H. Liu, T. Li, Z. G. Dong, S. N. Zhu, and X. Zhang, Phys. Rev. E **75**, 016604 (2007).
[8] T. Li, H. Liu, F. M. Wang, Z. G. Dong, S. N. Zhu, and X. Zhang, Opt. Express **14**, 11155 (2006).
[9] S. Zhang, W. Fan, N. C. Panoiu, K. J. Malloy, R. M. Osgood, and S. R. J. Brueck, Phys. Rev. Lett. **95**, 137404 (2005).
[10] G. Dolling, M. Wegener, C. M. Soukoulis, and S. Linden, Opt. Lett. **32**, 53 (2007).
[11] H. K. Yuan, U. K. Chettiar, W. Cai, A. V. Kildishev, A. Boltasseva, V. P. Drachev, and V. M. Shalaev, Opt. Express **15**, 1076 (2007).
[12] T. J. Yen, W. J. Padilla, N. Fang, D. C. Vier, D. R. Smith, J. B. Pendry, D. N. Basov, and X. Zhang, Science **303**, 1494 (2004).
[13] S. Linden, C. Enkrich, M. Wegener, J. Zhou, Th. Koschny, and C. M. Soukoulis, Science **306**, 1351 (2004).
[14] A. N. Grigorenko, A. K. Geim, H. F. Gleeson, Y. Zhang, A. A. Firsov, I. Y. Khrushchev, and J. Petrovic, Nature (London) **438**, 335 (2005).
[15] C. Enkrich, M. Wegener, S. Linden, S. Burger, L. Zschiedrich, F. Schmidt, J. F. Zhou, Th. Koschny, and C. M. Soukoulis, Phys. Rev. Lett. **95**, 203901 (2005).
[16] A. Ishikawa, T. Tanaka, and S. Kawata, Phys. Rev. Lett. **95**, 237401 (2005).
[17] G. Dolling, C. Enkrich, M. Wegener, J. F. Zhou, C. M. Soukoulis, and S. Linden, Opt. Lett. **30**, 3198 (2005).
[18] C. Luo, S. G. Johnson, and J. D. Joannopoulos, Appl. Phys. Lett. **81**, 2352 (2002).
[19] H. Shin and S. Fan, Appl. Phys. Lett. **89**, 151102 (2006).
[20] R. Gajic, R. Meisels, F. Kuchar, and K. Hingerl, Phys. Rev. B **73**, 165310 (2006).
[21] X. Fan, G. P. Wang, J. C. W. Lee, and C. T. Chan, Phys. Rev. Lett. **97**, 073901 (2006).
[22] P. B. Johnson and R. W. Christy, Phys. Rev. B **6**, 4370 (1972).
[23] H. Liu, D. A. Genov, D. M. Wu, Y. M. Liu, J. M. Steele, C. Sun, S. N. Zhu, and X. Zhang, Phys. Rev. Lett. **97**, 243902 (2006).
[24] O. Sydoruk, O. Zhuromskyy, and E. Shamonina, Appl. Phys. Lett. **87**, 072501 (2005).
[25] D. R. Smith, D. C. Vier, Th. Koschny, and C. M. Soukoulis, Phys. Rev. E **71**, 036617 (2005).